

Transition Metal Polyhydride Complexes. 11. Mechanistic Studies of the Cis to Trans Isomerization of the Iridium(III) Dihydride Ir(H)₂(CO)L (L = C₆H₃(CH₂P(H)₂)₂)

Shuhua Li and Michael B. Hall*

Department of Chemistry, Texas A&M University, College Station, Texas 77843

Received August 25, 1999

Density functional theory (B3LYP) has been used to investigate the mechanism of the cis–trans isomerization in Ir(H)₂(CO)L (L = C₆H₃(CH₂P(H)₂)₂), a model for Ir(H)₂(CO)L' (L' = C₆H₃(CH₂P(i-Pr)₂)₂). This complex is initially formed as the cis isomer by bubbling H₂ through a benzene solution of Ir(CO)L' at room temperature. Over period of 18 h at 90 °C, the cis isomer quantitatively converts to the trans isomer (*Organometallics* **1997**, *16*, 3786). Five possible mechanisms are examined in detail: (i) CO dissociation and reassociation; (ii) CO migratory insertion into the Ir–H bond and subsequent elimination; (iii) Ph–H reductive elimination to an arene intermediate and subsequent oxidative addition; (iv) phosphine dissociation, complex rearrangement, and phosphine reassociation; and (v) nondissociative trigonal twist. The preferred mechanism involves two consecutive trigonal twists in which the complex passes through a distorted octahedral intermediate.

Introduction

The oxidative addition of H₂ to transition metal centers has been intensively studied for decades.^{1–12} It has been generally recognized that this process may produce the dihydride adduct either directly or via a dihydrogen intermediate depending on the nature of the

transition metals and the ancillary ligands.¹ Examples of the latter include several reports on the kinetics and thermodynamics of the dihydrogen/dihydride equilibrium in some tungsten and rhenium complexes.^{13–16} However, if the cis-dihydride product, which is usually formed first in the H₂ addition process, is not thermodynamically stable, subsequent rearrangements may give another cis- or trans-dihydride complex. This concomitant process has not been thoroughly investigated either experimentally or theoretically.^{17–20} To the best of our knowledge, the rearrangement of a kinetically formed dihydride isomer to the thermodynamically stable dihydride isomer has been investigated experimentally in only three cases: M(H)₂(L)₄ (M = Fe, Ru; L = phosphorus donor),¹⁷ Ir(H)₂Br(CO)(dppe),¹⁸ and [C₅H₅B–Ph][C₄H₄B–N(i-Pr)₂]Ta(H)₂(PET₃).¹⁹ In the first case, an intramolecular nondissociative path, specifically the “tetrahedral jump”, was established by NMR line-shape analysis.¹⁷ For the second case, two competi-

- (1) (a) Heinekey, D. M.; Oldham, W. J., Jr. *Chem. Rev.* **1993**, *93*, 913. (b) Kubas, G. J.; Ryan, R. R.; Swanson, B. I.; Vergamini, P. J.; Wasserman, H. *J. Am. Chem. Soc.* **1984**, *106*, 451. (c) Kubas, G. J. *Acc. Chem. Res.* **1988**, *21*, 129. (d) Crabtree, R. H. *Acc. Chem. Res.* **1990**, *23*, 95.
- (2) (a) Kitaura, K.; Obara, S.; Morokuma, K. *Chem. Phys. Lett.* **1981**, *77*, 452. (b) Kitaura, K.; Obara, S.; Morokuma, K. *J. Am. Chem. Soc.* **1981**, *103*, 2891. (c) Kitaura, K.; Obara, S.; Morokuma, K. *J. Am. Chem. Soc.* **1984**, *106*, 7482.
- (3) (a) Noell, J. O.; Hay, P. J. *J. Am. Chem. Soc.* **1982**, *104*, 4578. (b) Hay, P. J. *J. Am. Chem. Soc.* **1987**, *109*, 705.
- (4) (a) Low, J. J.; Goddard, W. A., III. *J. Am. Chem. Soc.* **1984**, *106*, 6928. (b) Low, J. J.; Goddard, W. A., III. *Organometallics* **1986**, *5*, 609. (c) Low, J. J.; Goddard, W. A., III. *J. Am. Chem. Soc.* **1986**, *108*, 6115.
- (5) Brandemark, U. B.; Blomberg, M. R. A.; Petersson, L. G. M.; Siegbahn, P. E. M. *J. Phys. Chem.* **1984**, *88*, 4617.
- (6) Vaska, L. *Chem. Rev.* **1988**, *88*, 1147.
- (7) (a) Sargent, A. L.; Hall, M. B.; Guest, M. F. *J. Am. Chem. Soc.* **1992**, *114*, 517. (b) Lin, Z.; Hall, M. B. *J. Am. Chem. Soc.* **1992**, *114*, 2928. (c) Lin, Z.; Hall, M. B. *J. Am. Chem. Soc.* **1992**, *114*, 6102. (d) Lin, Z.; Hall, M. B. *Coord. Chem. Rev.* **1994**, *135/136*, 845. (e) Lin, Z.; Hall, M. B. *J. Am. Chem. Soc.* **1994**, *116*, 4446. (f) Bayse, C. A.; Hall, M. B.; Pleune, B.; Poli, R. *Organometallics* **1998**, *17*, 4309. (g) Bayse, C. A.; Couty, M.; Hall, M. B. *J. Am. Chem. Soc.* **1996**, *118*, 8916. (h) Bayse, C. A.; Hall, M. B. *Organometallics* **1998**, *17*, 4861.
- (8) (a) Abu-Hasanayn, F.; Krogh-Jespersen, K.; Goldman, A. S. *Inorg. Chem.* **1993**, *32*, 495. (b) Abu-Hasanayn, F.; Krogh-Jespersen, K.; Goldman, A. S. *J. Am. Chem. Soc.* **1993**, *115*, 8019. (c) Abu-Hasanayn, F.; Goldman, A. S.; Krogh-Jespersen, K. *J. Phys. Chem.* **1993**, *97*, 5890. (d) Abu-Hasanayn, F.; Goldman, A. S.; Krogh-Jespersen, K. *Inorg. Chem.* **1994**, *33*, 5122.
- (9) Ziegler, T.; Tschinke, V.; Fan, L.; Becke, A. D. *J. Am. Chem. Soc.* **1989**, *111*, 9177.
- (10) Wang, W.; Weitz, E. *J. Phys. Chem. A* **1997**, *101*, 2358.
- (11) Musaev, D. G.; Morokuma, K. *J. Am. Chem. Soc.* **1995**, *117*, 799.
- (12) (a) Macgregor, S. A.; Eisenstein, O.; Whittlesey, M. K.; Perutz, R. N. *J. Chem. Soc., Dalton Trans.* **1998**, 291. (b) Clot, E.; Eisenstein, O. *J. Phys. Chem. A* **1998**, *102*, 3592.

- (13) Chinn, M. S.; Heinekey, D. M.; Payne, N. G.; Sofield, C. D. *Organometallics* **1989**, *8*, 1824.

- (14) Luo, X. L.; Michos, D.; Crabtree, R. H. *Organometallics* **1992**, *11*, 237.

- (15) (a) Kubas, G. J.; Ryan, R. R.; Wroblewski, D. A. *J. Am. Chem. Soc.* **1986**, *108*, 1339. (b) Kubas, G. J.; Unkefer, C. J.; Swanson, B. I.; Fukushima, E. *J. Am. Chem. Soc.* **1986**, *108*, 7000.

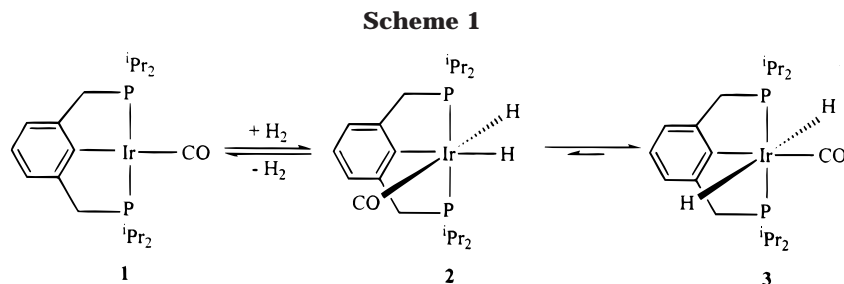
- (16) Khalsa, G. R. K.; Kubas, G. J.; Unkefer, C. J.; Stepan Van Der Sluis, L. *J. Am. Chem. Soc.* **1990**, *112*, 3855.

- (17) (a) Meakin, P.; Guggenberger, L. J.; Jesson, J. P.; Gerlach, D. H.; Tebbe, F. N.; Peet, W. G.; Muettterties, E. L. *J. Am. Chem. Soc.* **1970**, *92*, 3482. (b) Gerlach, D. H.; Peet, W. G.; Muettterties, E. L. *J. Am. Chem. Soc.* **1972**, *94*, 4545. (c) Meakin, P.; Muettterties, E. L.; Tebbe, F. N.; Jesson, J. P. *J. Am. Chem. Soc.* **1971**, *93*, 4701. (d) Meakin, P.; Muettterties, E. L.; Jesson, J. P. *J. Am. Chem. Soc.* **1973**, *95*, 75.

- (18) Kunin, A. J.; Johnson, C. E.; Maguire, J. A.; Jones, W. D.; Eisenberg, R. *J. Am. Chem. Soc.* **1987**, *109*, 2963.

- (19) Sperry, C. K.; Bazan, G. C.; Cotter, W. D. *J. Am. Chem. Soc.* **1999**, *121*, 1513.

- (20) Paonessa, R. S.; Trogler, W. C. *J. Am. Chem. Soc.* **1982**, *104*, 1138.

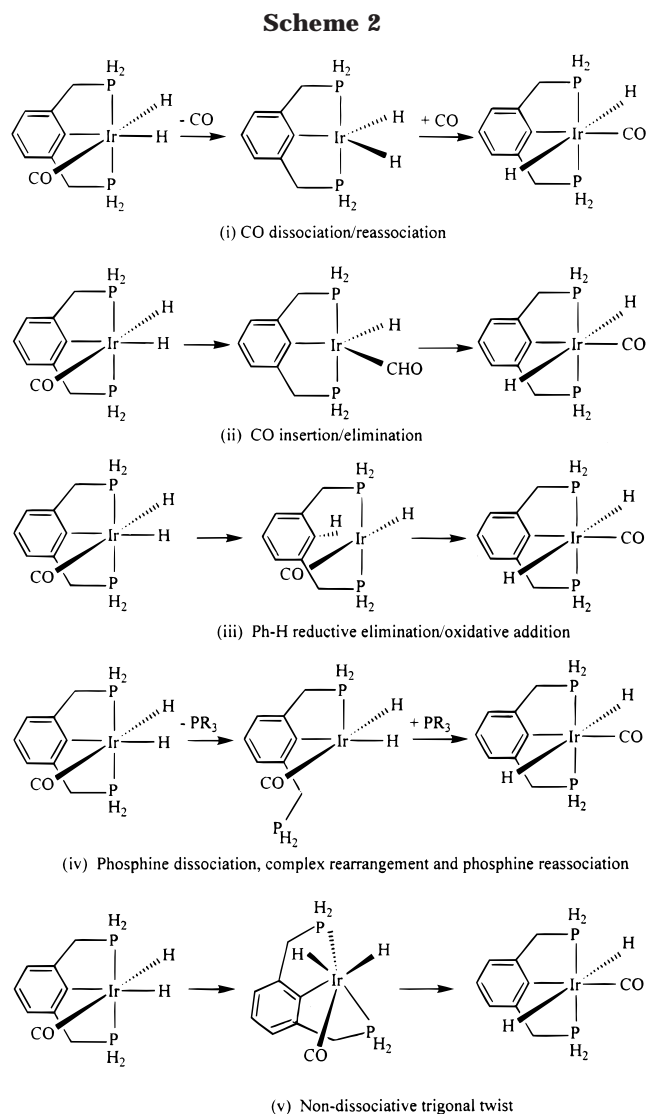


tive mechanisms including a dihydride reductive-elimination, oxidative-addition pathway and a bimolecular process were found to be responsible for the isomerization.¹⁸ In the third case, a phosphine dissociation followed by the rearrangement of the remaining intermediate prior to phosphine recoordination was proposed.¹⁹ From these examples, one can see the diversity of isomerization mechanisms in dihydride complexes. In addition to these systems, the cis–trans isomerization of platinum(II) dihydrides has also been observed, but the detailed mechanism is unknown.²⁰ Recently, the kinetically formed octahedral iridium cis-dihydride $\text{Ir}(\text{H})_2(\text{CO})\text{L}'$ ($\text{L}' = \text{C}_6\text{H}_3(\text{CH}_2\text{P}(\text{i-Pr})_2)_2$) (**2**) was found by Rytchinski, Ben-David, and Milstein²¹ to quantitatively convert into the corresponding trans-dihydride complex **3** after 18 h at 90 °C under the protection of 35 psi of H_2 (H_2 was added to prevent the formation of **1** from **2**) (Scheme 1). A mechanism for the isomerization reaction was not discussed in this work.

In this paper, we investigate this cis–trans isomerization in the model system $\text{Ir}(\text{H})_2(\text{CO})\text{L}$ ($\text{L} = \text{C}_6\text{H}_3(\text{CH}_2\text{P}(\text{H})_2)_2$) by density functional theory. Five possible pathways (Scheme 2) are examined in detail: (i) CO dissociation and reassociation; (ii) CO migratory insertion into the Ir–H bond and subsequent elimination; (iii) Ph–H reductive elimination to an arene intermediate and subsequent oxidative addition; (iv) phosphine dissociation, complex rearrangement, and phosphine reassociation; and (v) nondissociative trigonal twist.

Computational Details

All the calculations have been performed with the Gaussian 94²³ package. Density functional theory²⁴ was employed with the three-parameter hybrid exchange functional of Becke²⁵ and the Lee, Yang, and Parr correlation functional²⁶ (B3LYP). Relativistic effective core potentials (ECPs)²⁷ for iridium and phosphorus were employed in all B3LYP calculations. In the ECP for Ir, the 5s and 5p orbitals were treated explicitly along with the 5d, 6s, and 6p valence orbitals. The basis set for Ir



was a double- ζ basis set (341/541/21), where the two outermost 6p functions of the standard LANL2DZ²⁸ have been replaced by a (41) split of the optimized 6p function from Couty and Hall.²⁹ For P, the standard LANL2DZ basis set was augmented by a d-type polarization function.³⁰ For metal-bound carbon and hydrogen atoms and for the oxygen atom, a 6-31G(d,p) basis set³¹ was adopted. The hydrogen and carbon atoms uncoordinated to the metal have a 3-21G basis set.³²

(28) LANL2DZ: Dunning D95 basis sets on first row, Los Alamos ECP plus double- ζ basis sets on Na–Bi.

(29) Couty, M.; Hall, M. B. *J. Comput. Chem.* **1996**, *17*, 1359.

(30) Höllwarth, A.; Böhme, M.; Dapprich, S.; Ehlers, A. W.; Gobbi, A.; Jonas, V.; Köhler, K. F.; Stegmann, R.; Veldkamp, A.; Frenking, G. *Chem. Phys. Lett.* **1993**, *208*, 237.

(31) Harihan, P. C.; Pople, J. A. *Theor. Chim. Acta* **1973**, *28*, 213.

(32) Hehre, W. J.; Radom, L.; Schleyer, P. v. R.; Pople, J. A. *Ab initio molecular orbital theory*; Wiley: New York, 1986.

(21) Rytchinski, B.; Ben-David, Y.; Milstein, D. *Organometallics* **1997**, *16*, 3786.

(22) Bailar, J. C., Jr. *J. Inorg. Nucl. Chem.* **1958**, *8*, 165.

(23) Frisch, M. J.; Trucks, G. W.; Schlegel, H. B.; Gill, P. M. W.; Johnson, B. G.; Robb, M. A.; Cheeseman, J. R.; Keith, T.; Petersson, G. A.; Montgomery, J. A.; Raghavachari, K.; Al-Laham, M. A.; Zakrzewski, V. G.; Ortiz, J. V.; Foresman, J. B.; Peng, C. Y.; Ayala, P. Y.; Chen, W.; Wong, M. W.; Andres, J. L.; Replogle, E. S.; Gomperts, R.; Martin, R. L.; Fox, D. J.; Binkley, J. S.; Defrees, D. J.; Baker, J.; Stewart, J. P.; Head-Gordon, M.; Gonzalez, C.; Pople, J. A. *Gaussian 94*, Revision B.3; Gaussian Inc.: Pittsburgh, PA, 1994.

(24) Parr, R. G.; Yang, W. *Density-functional theory of atoms and molecules*; Oxford University Press: Oxford, 1989.

(25) (a) Becke, A. D. *Phys. Rev.* **1988**, *A38*, 3098. (b) Becke, A. D. *J. Chem. Phys.* **1993**, *98*, 1372. (c) Becke, A. D. *J. Chem. Phys.* **1993**, *98*, 5648.

(26) Lee, C.; Yang, W.; Parr, R. G. *Phys. Rev.* **1988**, *B37*, 785.

(27) (a) Hay, P. J.; Wadt, W. R. *J. Chem. Phys.* **1985**, *82*, 299. (b) Wadt, W. R.; Hay, P. J. *J. Chem. Phys.* **1985**, *82*, 284.

All intermediates and transition states (TS) in this work were obtained by full geometry optimizations at the B3LYP level. The transition states, checked by separate frequency calculations, have only one imaginary frequency.

Results and Discussion

In this section, we begin with a description of the geometrical features of the cis- and trans-dihydride model complexes. Then each of the five mechanisms will be discussed at some length in a separate subsection. To save space, the structures of all optimized intermediates and transition states obtained along the five possible pathways are collected in Figure 1, and their relative electronic energy differences are tabulated in Table 1. Since the relative zero-point-energy differences generally have a very small influence on the relative heights of activation barriers for isomerizations, their values are not included in Table 1.

By replacing *i*-Pr substituents with hydrogens in **2** and **3**, we obtain the model species **4** and **5**, respectively. The energies in Table 1 show that the trans-dihydride **5** is lower in energy than the cis isomer **4** by 2.0 kcal/mol, a value that is in agreement with the experimental estimate for the energy difference between **2** and **3** ($\Delta G_{2-3}(363\text{ K}) = G_3 - G_2 \leq -3.3\text{ kcal/mol}$).²¹

This energy difference seems to contradict the well-known fact that a hydride ligand has a stronger trans-influence than a phenyl (Ph) ligand. The optimized structures for **4** and **5**, which are given in Figure 1, provide some clues about the relative stability of the trans-dihydride **5** over the cis-dihydride **4**. By comparing the Ir–C2 (Ir–CO) bond distances trans to the hydride in **4** (1.933 Å) and the Ph group in **5** (1.914 Å), we find the expected trans-influence trend H > Ph. So what are the factors that contribute to the stabilization of **5** over **4**? Are there some electronic factors that favor the trans arrangement of two hydrides in **5** even though this arrangement is usually unfavorable?^{7h} Analyzing the occupied molecular orbitals of **5**, we note a delocalized interaction between the π orbitals of Ph, the d_π of Ir, and the π orbitals of CO (these orbitals are nearly in the same plane). Apparently, this electron delocalization favors Ph trans to CO, the isomer in which both the Ir–Ph and Ir–CO bonds are shorter. This viewpoint can be indirectly substantiated by comparing the relative stability of two model complexes, cis- and trans-Ir(H)₂(CO)(CH₃)(PH₂)₂, in which the Ph group in **4** and **5** has been replaced with the simple methyl group. Full geometry optimizations at the B3LYP level (not listed here) show that the trans isomer is slightly higher in energy than the cis one. Clearly, the reason can be ascribed to the fact that the stabilizing delocalization in **5** is partially reduced in *trans*-Ir(H)₂(CO)(CH₃)(PH₂)₂ because the CH₃ group lacks the delocalized π system of Ph. Interestingly, the isomer with the shorter Ir–CO bond, **5**, has the longer C–O bond, a result that is in agreement with the C–O stretching frequencies.²¹ In addition, examining the geometrical features of **4** and **5**, we find that ring strain may destabilize **4** to some extent. As one can see from Figure 1, both five-membered rings in **5** are equally twisted (in opposite directions) to relieve some strain energy. Both dihedral angles, P1–Ir–C1–C3 and P2–Ir–C1–C4, are -15.3° in **5**. However, in **4** only the upper five-membered ring

is twisted to the same extent as that in **5** (the dihedral angle P1–Ir–C1–C3 is -15.6°). The lower ring is puckered to a smaller extent (the dihedral angle P2–Ir–C1–C4 is -8.2°). These strain effects could be more important when bulky substituents are attached to P.

CO Dissociation/Reassociation. The reaction coordinate along this pathway is shown schematically in Figure 2.

After CO dissociation, the most stable five-coordinate intermediate is **6**, a distorted trigonal bipyramid with a small H–Ir–H angle (see Figure 1). For isomerization, CO reassociation would occur with the less stable intermediate **7**, a square pyramid with two hydrides trans to each other. Since the barrier for CO dissociation is at least 40.5 kcal/mol, this mechanism can be eliminated as having a barrier too large to explain the experimental results. Although the basis set superposition error (BSSE) is not included, it will not be large enough to change this conclusion.

CO Insertion/Elimination. Although CO insertion into a M–H bond is generally unfavorable thermodynamically, it does occur in some transition metal systems.³³ So this pathway could be a possibility for the isomerization. The calculated potential energy profile is given in Figure 3. From Figures 1 and 3, we can see that the first step along this mechanism is the migration of the hydride H1 to the CO, **8**(TS), and then the CHO group moves to form a trigonal bipyramidal acyl intermediate **9**. Finally, the CO is eliminated from **9** to generate the trans-dihydride product **5**. Although the CO elimination from the intermediate **9** to form the product **5** is facile with a barrier of only 9.2 kcal/mol, the CO insertion step is endothermic by 25.3 kcal/mol with a barrier of 39.6 kcal/mol. Therefore, this mechanism is also an unsuitable explanation for the experimental observation.

The instability of **9** relative to the cis-dihydride **4** is due to a combination of factors. Although a very strong C2–H1 bond is created in **9**, three other factors combine to destabilize **9** (compared to **4**): (i) the strong Ir–H1 bond is completely broken in **9**; (ii) the triple bond of CO in **4** is reduced to a double bond in **9**, as evidenced by the C–O bond lengthening from 1.156 to 1.212 Å; and (iii) the Ir–C2 bond in **9** is significantly weaker, as reflected in its elongation by 0.025 Å.

Ph–H Reductive-Elimination/Oxidative-Addition. The potential energy path for this mechanism is shown in Figure 4. First, the Ir–H2 and Ir–C1 bonds reductively eliminate to form intermediate **12** (see Figure 1), then the arene ring twists to produce intermediate **14**, and finally the C1–H2 bond oxidatively adds to generate the trans-dihydride **5**. The calculated barriers for these three consecutive steps are 33.2, 18.6, and 16.4 kcal/mol, respectively. Clearly, the Ph–H reductive elimination from **4** to **12** is the rate-determining step along this pathway, and its barrier of 33.2 kcal/mol is still too high to interpret the experimental observation.

The optimized transition states and intermediates along this path (see Figure 1) deserve some comments.

(33) (a) Fagan, P. J.; Moloy, K. G.; Marks, T. J. *J. Am. Chem. Soc.* **1981**, *103*, 6959. (b) Wayland, B. B.; Woods, B. A. *J. Chem. Soc., Chem. Commun.* **1981**, 700.

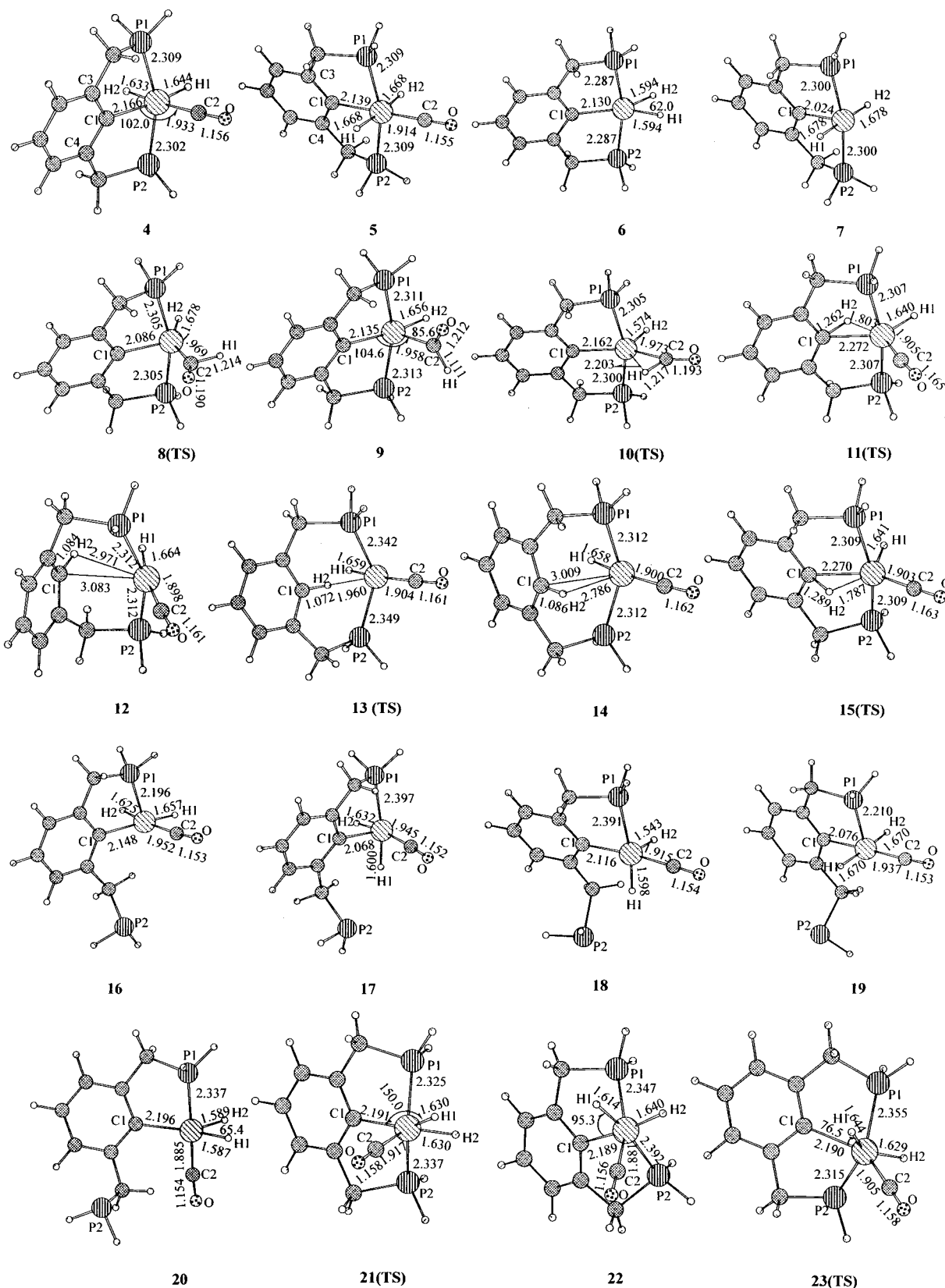


Figure 1. B3LYP-optimized structures of the reactant **4**, the product **5**, and all of the intermediates and transition states along the five possible pathways.

The geometrically similar intermediates, **12** and **14**, are only 12.5 and 11.5 kcal/mol, respectively, above the reactant **4**. Both intermediates are actually four-coordinate Ir(I) (d^8) complexes because of the reductive elimination of the Ir–H2 and Ir–C1 bonds. Despite the loss of two bonds and the gain of only one, **12** and **14**

are reasonably stable because the newly formed C1–H2 bond is strong, the Ir–C2 bond is stronger than that in **4**, and part of the ring strain is released. On the other hand, the barrier for the reductive elimination is relatively high because in the transition state **11** (also **15**) Ir–C1 and Ir–H2 bond breaking costs more energy

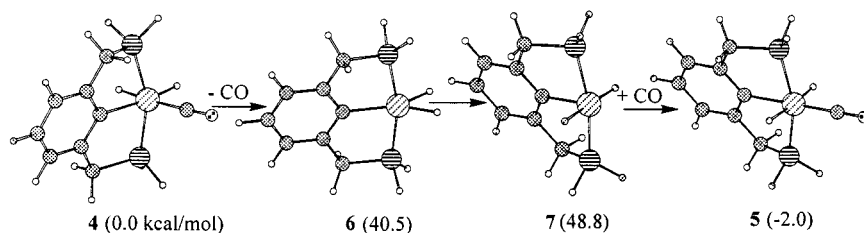


Figure 2. Potential energy profile along the CO dissociation/reassociation pathway. Only the energies of intermediates are given because of the high dissociation energy in the first step.

Table 1. Relative Electronic Energies ΔE (in kcal/mol) of the Reactant 4, Intermediates, Transition States, and the Product 5

species ^a	ΔE	species ^a	ΔE
4	0.0	14	11.52
5	-2.01	15(TS)	27.91
6 + CO^b	40.51	16	46.64
7 + CO^b	48.77	17	35.52
8(TS)	39.64	18	25.41
9	25.25	19	42.58
10(TS)	34.48	20	31.01
11(TS)	33.23	21(TS)	24.04
12	12.49	22	7.95
13(TS)	31.06	23(TS)	24.03

^a See the numbering of species in Figure 1. The transition states are explicitly denoted in parentheses. ^b The basis set superposition error is not included.

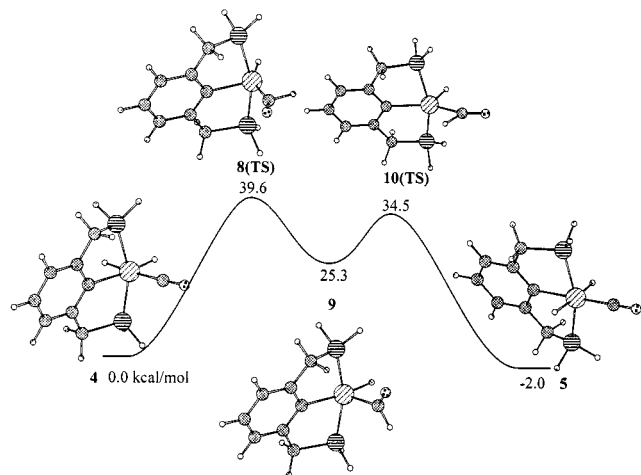


Figure 3. Potential energy profile along the CO insertion/elimination pathway.

than that returned from C1–H2 bond forming and the ring strain is still large.

Phosphine Dissociation, Complex Rearrangement, and Phosphine Reassociation. The sequence of phosphine dissociation, complex rearrangement, and phosphine reassociation is quite complicated because there are a number of rearrangement modes for the resultant five-coordinate complex **16** before the phosphine group recoordinates to the metal center to yield the trans-dihydride product **5**. For example, the **4** \rightarrow **5** cis–trans isomerization could go through the reaction coordinate shown in Figure 5 (the relative electronic energies of these intermediates are also listed for comparison). Obviously, without simultaneous rearrangements of other ligands the direct Ir–P bond breaking from **4** to **16** is highly endothermic (46.6 kcal/mol). Thus, the mechanism displayed in Figure 5 can be definitively excluded.

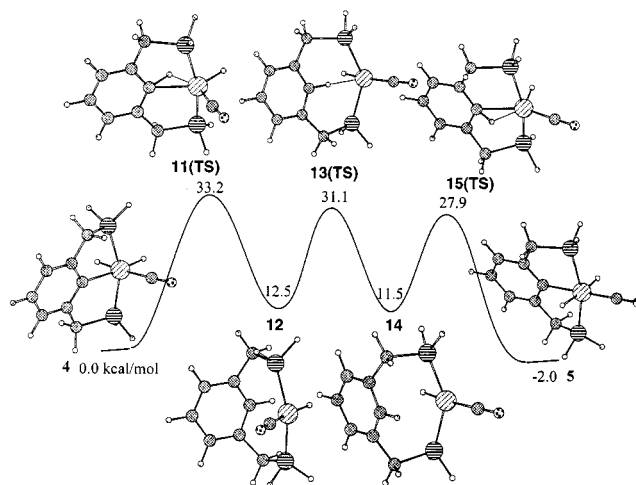


Figure 4. Potential energy profile along the Ph–H reductive-elimination, oxidative-addition reaction coordinate.

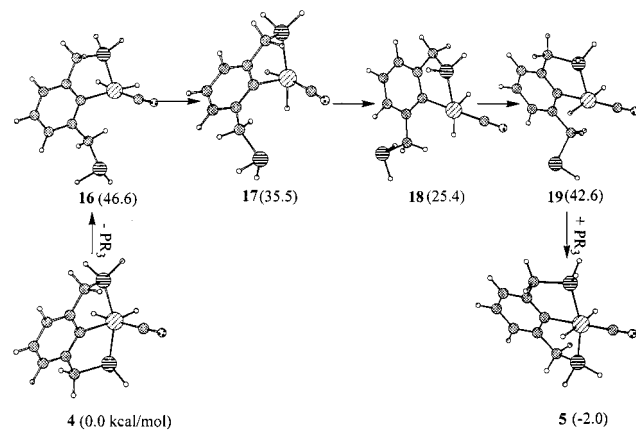


Figure 5. Potential energy profile along a phosphine dissociation, complex rearrangement, and phosphine reassociation pathway. Only the energies of intermediates are given because of the high dissociation energy in the first step.

However, simultaneous rearrangement of the remaining ligands as the phosphine dissociates is possible. Apparently, phosphine dissociation from **4** directly to **17** or **20** is also highly unfavorable thermodynamically, but direct dissociation to **18**, in which one hydride ligand is trans to a vacant site, would produce the most stable among possible five-coordinate intermediates. In an attempt to find such a route, we performed several restricted geometry optimizations by fixing the Ir–P2 to 3.0 Å, a value that is halfway between the normally coordinated and the completely dissociated limits, and by starting from various initial geometries, which are constructed by moving one or more of the remaining ligands (H1, H2, CO) slightly away from their original

positions. These optimizations all converged to the same structure, which is 26.5 kcal/mol above the reactant **4** and geometrically very similar to **16** (except of course in the one Ir–P bond length). Therefore, even if a direct path from **4** to **18** exists, the activation barrier for the loss of the phosphine ligand along this path will be greater than 26.5 kcal/mol. Experiments also suggest that phosphine loss is not facile: a complex like **5** is stable under 30 psi of CO at 50 °C,²¹ and complexes like **6** are stable up to 200 °C.³⁴ As we will see in the following section, another pathway is lower in energy than this minimum value for phosphine dissociation, complex rearrangement, and phosphine reassociation.

Trigonal Twist. Nondissociative mechanisms have been unequivocally determined to be responsible for the stereochemical nonrigidity only in a few octahedral or distorted-octahedral six-coordinate molecules.^{17,35,36} There are three well-known kinds of nondissociative rearrangement modes in six-coordinate molecules, distinguished by the geometrical character of the transition state: (i) the tetrahedral jump mechanism,¹⁷ (ii) the bicapped tetrahedral mechanism,³⁷ and (iii) the trigonal twist mechanism²² (see related references for details). Let us return to the specific isomerization in our case. First, the tetrahedral jump mechanism in our case means that species **4** may isomerize into **5** through a single H1 jump across the P1–C2 edge with concomitant movement of CO ligand to the position trans to the phenyl ligand (see Figure 1). Our search for a transition state primarily involving the H1 movement did lead to a transition state, **21** in Figure 1. However, **4** to **21** also involves large movements of the H2 and P1 ligands and thus does not appear to be a tetrahedral jump. Furthermore, intrinsic reaction coordinate (IRC)³⁸ calculations show that this transition state does not directly connect **4** and **5**. In fact, as we will show, species **21** is a transition state along the trigonal twist pathway. Therefore, the tetrahedral jump mechanism can be ruled out as a possibility.

By the bicapped tetrahedral mechanism, the isomerization from **4** to **5** can occur in a single step by rotating H1 and CO ligands simultaneously in **4**. We have made an extensive search for transition states along this path. Interestingly, we indeed located another transition state, **23** in Figure 1. Again, an IRC calculation shows that this transition state fails to connect the reactant **4** and the product **5**. Thus, the bicapped tetrahedral mechanism is also excluded.

Now, the trigonal twist process is only the nondissociative pathway left to be explored. Following this path, we have obtained the intermediate **22** (Figure 1) and two transition states **21** and **23**, both mentioned above. The potential energy profile associated with this path is provided in Figure 6. The intermediate **22** is a

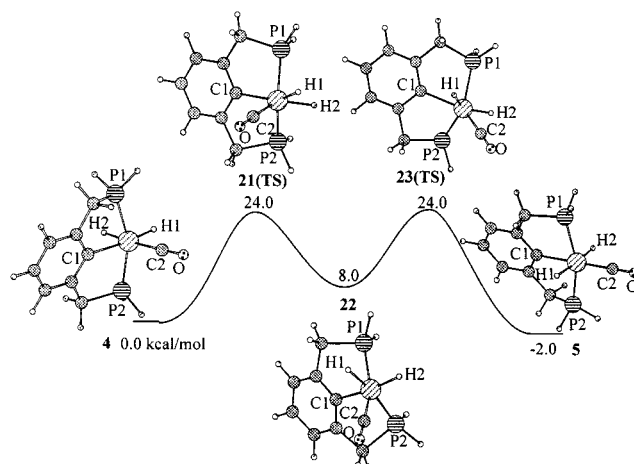


Figure 6. Potential energy profile along the trigonal twist pathway.

distorted octahedral complex that is generated from **4** by twisting the three ligand atoms: P1, H2, and H1 simultaneously. The trans-dihydride product **5** is then obtained by rotating the three ligand atoms, C2, H2, and P2, in the intermediate **22**. The trigonal prismatic transition states **21** and **23** have been verified by subsequent IRC calculations to truly connect **4** to **22** and **22** to **5**, respectively. Since the barriers for these two consecutive trigonal twist rotations are only 24.0 and 16.0 kcal/mol, respectively, the trigonal twist process turns out to be the lowest energy pathway among the five reaction mechanisms under consideration. The activation parameters we obtained along the trigonal twist mechanism are in reasonable accord with the experimental conditions in which the real cis-dihydride complex **2** isomerizes into the trans-dihydride **3**.

Conclusions

Density functional theory provides the mechanism, structures, and energetics involved in the isomerization of the cis-dihydride complex Ir(H)₂(CO)L (L = C₆H₃-(CH₂P(H)₂)₂) into its trans-dihydride counterpart, which is thermodynamically more stable. Five possible mechanisms have been investigated in detail. The favored mechanism is two consecutive trigonal twists through a distorted octahedral intermediate. The low energy of this path is unexpected because of the backbone rigidity of the tridentate ligand –C₆H₃(CH₂PR₂)₂. The calculated activation parameters are in agreement with the reaction conditions in which the cis–trans isomerization in analogous real dihydride complex Ir(H)₂(CO)L' (L' = C₆H₃(CH₂P(i-Pr)₂)₂) occurs. Since all of the other four mechanisms have higher barriers, our theoretical calculations provide strong evidence that the isomerization reaction observed above proceeds by the trigonal twist mechanism.

Acknowledgment. We would like to thank the National Science Foundation (Grant No. CHE 9800184) and the Robert A. Welch Foundation (Grant No. A-648) for their generous support.

OM9906868

(34) Xu, W.-w.; Rosini, G. P.; Gupta, M.; Jensen, C. M.; Kaska, W. C.; Krogh-Jespersen, K.; Goldman, A. S. *J. Chem. Soc., Chem. Commun.* **1997**, 2273.

(35) Ball, G. E.; Mann, B. E. *J. Chem. Soc., Chem. Commun.* **1992**, 561.

(36) Bayse, C. A.; Couty, M.; Hall, M. B. *J. Am. Chem. Soc.* **1996**, *115*, 8916.

(37) Hoffmann, R.; Howell, J. M.; Rossi, A. R. *J. Am. Chem. Soc.* **1976**, *98*, 2484.

(38) Gonzalez, C.; Schlegel, H. B. *J. Phys. Chem.* **1990**, *94*, 55.